The Astrophysical Journal, 647:1375–1386, 2006 August 20

ROTATIONAL AND CYCLICAL VARIABILITY IN γ CASSIOPEIA

Myron A. Smith
Catholic University of America, 3700 San Martin Drive, Baltimore, MD 21218; msmith@stsci.edu

Gregory W. Henry
Center of Excellence in Information Systems, Tennessee State University, 3500 John A. Merritt Boulevard, Nashville, TN 37209; henry@schwab.tsuniv.edu

and

Ethan Vishniac
Department of Physics and Astronomy, Johns Hopkins University, 3400 North Charles Street, Baltimore, MD 21218; ethan@pha.jhu.edu
Received 2005 December 8; accepted 2006 April 29

ABSTRACT

γ Cas is an unusual classical Be star for which the optical-band and hard X-ray fluxes vary on a variety of timescales. We report results of a 9 yr monitoring effort on this star with a robotic ground-based (APT) telescope in the *B*, *V* filter system, as well as simultaneous observations in 2004 November with this instrument and the *RXTE*. Our observations disclosed no correlated optical response to the rapid X-ray flares in this star, nor did the star show any sustained flux changes any time during two monitored nights in either wavelength regime. Consistent with an earlier study by Robinson et al., optical light curves obtained in our new APT program revealed that γ Cas undergoes $\sim$3% amplitude cycles with lengths of 50–91 days. Our observations in 2004 showed a similar optical cycle. Over the 9 days we monitored the star with the *RXTE*, the X-ray flux varied in phase with its optical cycle and with an amplitude predicted from the data in Robinson et al. In general, the amplitude of the *V* magnitude cycles are 30%–40% larger than the corresponding *B* amplitude, suggesting that the production site of the cycles is circumstellar. The cycle lengths constantly change and can damp or grow on timescales as short as 13 days. We have also discovered a coherent period of 1.21581 ± 0.00004 days in all our data, which appears consistent only with rotation. The full amplitude of this variation is 0.0060 in both filters, and, surprisingly, its waveform is almost sawtooth in shape. This variation is likely to originate on the star's surface. This circumstance hints at the existence of a strong magnetic field with a complex topology and a possible heterogeneous surface distribution of metals.

Subject headings: stars: emission-line, Be — stars: individual (γ Cassiopeia) — X-rays: stars

Online material: machine-readable table

1. INTRODUCTION

Discovered as the first of its class in 1867, γ Cas (B0.5 IV) is by definition the prototype of "classical Be stars."[1] Its strong Hα emission arises from a disk that is among a handful that have been observed in the infrared, millimeter, and centimeter radio regions. Its emission is due in large part to the disk's high central density of 10^{13} cm^{-3}, which is among the highest known for classical Be stars (e.g., Waters et al. 1987). The disk has been imaged interferometrically in Hα flux by several groups (e.g., Quirrenbach et al. 1997; Tycner et al. 2004) out to a distance of at least $6R_*$. Measurements of the ratio of the semiminor to semimajor axis of this image permit estimates of the rotational inclination of the star/disk rotational axis: $i = 46^\circ$ and 60°, respectively. Berio & Stée (1999) have imaged a dense azimuthal sector of the disk that orbited the star with a period of several years. This structure is likely due to a one-armed density pattern that develops in perhaps one-fourth of all Be stars (Hummel 2000) and is responsible for the oscillating ratio of the *V* and *R* Hα emission components in many of these stars. The effect of the star's radiative wind and stellar disk on its immediate environment is yet to be determined. Recently, Harmanec et al. (2000) and Miroschnichenko et al. (2002) have found that γ Cas is in a 204 day binary with a low eccentricity. The evolutionary status of the low-mass secondary is unknown. Given the orbital separation of this system, it is possible that the gravitational perturbations from the secondary are important in truncating the outer edge of the disk (Okazaki & Negueruela 2001).

Although γ Cas is typical for a Be star in most of these respects, it is highly unusual in others. Chief among its peculiarities is a rich array of variability patterns in the optical, ultraviolet, and X-ray regimes that extend from timescales of seconds to years (e.g., Horaguchi et al. 1994; Harmanec 2002). A proper understanding of the interrelationship between these variabilities requires a series of dedicated time sequences of observations in both wavelength domains. This paper represents a continuation of a series of efforts dedicated to determining how these various patterns are related using simultaneous or contemporaneous satellites, including the Goddard High Resolution Spectrograph (GHRS) attached to the *Hubble Space Telescope* (*HST*), the *Rossi X-Ray Timing Explorer* (*RXTE*), and the *International Ultraviolet Explorer* (*IUE*).

The coordinated X-ray prong of this campaign consisted of a simultaneous 22 hr monitoring in 1996 January with the GHRS and *RXTE*. A quasi-continuum light curve generated from the GHRS spectra exhibited a pair of 1%–2% dips over a few hours. The simultaneous *RXTE* fluxes showed maxima at these same times (Smith et al. 1998a). Subsequent analysis showed that the ultraviolet dips cannot arise on the Be star's surface and are most likely to occur from corotating "clouds" close to the star's surface (Smith et al. 1998b, hereafter SRH98). The same ultraviolet

[1] Here we define a classical Be star succinctly as an effectively isolated, post-ZAMS Be star, which has expelled matter that has settled into a disk confined to the rotational plane.

spectra showed many sharp features similar to the long-known blue-to-red "migrating subfeatures" (MSFs) in the star's optical line profiles (Yang et al. 1988; Smith 1995; Smith & Robinson 1999). A broad conclusion emerging from this program was that the immediate circumstellar environment of γ Cas, even beyond the equatorial plane, is highly complex. The system of corotating clouds (some heated and some cooled) alone constitutes a more complex environment than is indicated for most, if not all, other Be stars. Moreover, the clouds require a mechanism to anchor them onto fixed points on the surface. Such a mechanism may be presumed to be a strong magnetic field, but the discovery of a postulated field in this rapidly rotating star seems beyond the reach of present spectropolarimetric detection devices. This fact suggests that one must search for indirect indicators of magnetic field that can test this picture.

Accordingly, in 1997 Robinson et al. (2002, hereafter RSH02) mounted a long-term robotic photometric monitoring campaign on this star in the Johnson B and V system using an Automated Photometric Telescope (APT) in Arizona. Our program was to search for optical signatures of activity unique to γ Cas and especially for those correlated with known X-ray activity over a range of timescales. These included the rotational timescale, estimated to be near 1 day, as well as longer term variations that the *RXTE* campaigns and earlier observations on other X-ray satellites had suggested are present. Soon after they initiated this program, RSH02 identified a strong pattern characterized as small-amplitude, long (55–93 days) cycles. The fluxes from eight *RXTE* observations matched these cycles in length and phase but with nearly 100 times larger amplitudes. Because the energy associated with the optical variations is much larger than in the X-ray variations, this correlation cannot be interpreted simply as a reprocessing of the X-ray modulation, and one must seek another explanation. One clue to this interpretation is that the optical variations have a color consistent with the brightening/color trajectories that accompany the evolution of the disks of γ Cas and other Be stars. This fact suggests that the optical variations arise in the disk. Based on both the cyclicity and redness of the optical variations, RSH02 conjectured that both the optical variations and the generation of anomalous X-rays in γ Cas were produced by a Balbus-Hawley instability (Balbus & Hawley 1991), leading to a disk dynamo. Furthermore, the winding up of putative field lines from the star with the interaction of the Keplerian disk would stretch and sever their connections. The ensuing reconnections would accelerate disk atoms in the form of high-energy beams, which would generate X-rays when they impacted the surface of the Be star. The observation of absorption systems redshifted to 2000 km s^{-1} in the GHRS spectra (Smith & Robinson 2000) is consistent with the geometric and kinematic requirements of this speculative picture.

This paper presents the results of searches for rapid- and intermediate-timescale correlations of optical and X-ray fluxes of γ Cas. In § 4 we describe new characteristics of the long-term cycles found by RSH02 from nine seasons of optical robotic data. In § 5 we report the results of a successful search from this data set for a periodicity consistent with the star's expected rotational period and discuss its implications for models of this star's X-ray emission.

2. OBSERVATIONS

2.1. *Optical Data*

The optical photometry discussed in this paper was acquired with the T3 0.4 m APT, located at Fairborn Observatory in southern Arizona. The photometer uses a temperature-stabilized EMI 9924B photomultiplier tube to acquire data successively in the Johnson B and V filter passbands. The observations of γ Cas were acquired in the following sequence, termed a group observation: K, sky, C, V, C, V, C, V, C, sky, K, where K is the check star HD 5395 ($V = 4.62$, $B - V = 0.96$, G8 IIIb), C is the comparison star HD 6210 ($V = 5.83$, $B - V = 0.57$, F6 V), and V is the program star γ Cas ($V = 2.15$, $B - V = -0.05$, B0.5 IV). To avoid saturating the photomultiplier tube when observing γ Cas, we made the observations through a 3.8 mag neutral density filter. We used 10 s integration times for γ Cas and HD 5395 and 20 s for HD 6210 and the sky readings.

Three variable-minus-comparison and two check-minus-comparison differential magnitudes in each photometric band were computed for each group observation and then averaged to create group-mean differential magnitudes. The group means were corrected for differential extinction with nightly extinction coefficients, transformed to the Johnson system with yearly mean transformation coefficients, and treated as single observations thereafter. Typically, several group observations were made each clear night at intervals of approximately 2 hr. The external precision of the group means, based on standard deviations for pairs of constant stars, is typically ± 0.004 mag. However, point-to-point observations on intensively monitored nights were found to have a mean deviation of only ± 0.003 mag. Group means with a standard deviation greater than 0.01 mag were discarded. Further details of telescope operations and data reduction procedures can be found in Henry (1995a, 1995b).

Our photometric γ Cas observing program began in 1997 September and at this writing is ongoing. Our cutoff date for reporting data in this paper is 2006 February. Typically, we succeeded in obtaining a few nights of data at the beginning of each observing season in June before the Arizona rainy season forced us to close the APT operations for the summer, beginning around July 4 each year. We resumed the monitoring of γ Cas in mid-September each year and continued through the end of each observing season in February. Our observations during the first observing season between 1997 September and 1998 February (JD 2,450,718 through 2,450,856) were made using different neutral density filters for γ Cas and the other stars in the group. We found it difficult to calibrate the final reduced magnitudes properly. Therefore, these first-season observations have an undetermined offset with respect to observations in the rest of the seasons. The instrumental setup was stable for observing seasons 2 (1998–1999) through 9 (2005–2006). Our data set over nine seasons includes 3157 B and 3135 V observations. A sample of our differential magnitudes is tabulated in Table 1. The full data set is available in the online version of this paper. (An entry of "99.999" signifies that a differential magnitude was discarded because its internal standard deviation exceeded 0.01 mag, indicating nonphotometric conditions.) For plotting purposes, we added to our differential magnitudes the apparent V and B magnitudes of the comparison star ($m_V = 5.84$ and $m_B = 6.40$, respectively; after Breger 1974) to establish the proper zero point for our measures of γ Cas.

Beginning in the 2000–2001 season, we made an effort to dedicate occasional full nights ($\approx$8 hr) to the γ Cas program. A major effort to observe this star simultaneously with the *RXTE* satellite consisted of our attempting to observe intensively during the nights just preceding and following four coordinated nights in 2004 November, as well as the nights themselves. Altogether, 13 nights of the sustained monitorings are included in our data set, as well as several other nights of 5 hr or longer. The cadence rate of these intensive observations was one group cycle every 8 to 4 minutes.

TABLE 1
PHOTOMETRIC OBSERVATIONS OF γ CASSIOPEIA

Date (HJD − 2,400,000)	Var B (mag)	Var V (mag)	Chk B (mag)	Chk V (mag)
50711.7151	99.999	99.999	−0.822	99.999
50718.6966	−4.393	−3.641	−0.818	−1.216
50718.9253	−4.393	−3.642	−0.814	−1.222
50720.7936	−4.386	−3.644	−0.821	−1.218
50720.9191	−4.387	−3.638	99.999	−1.223
50721.6940	99.999	−3.648	99.999	99.999

NOTE.—Table 1 is published in its entirety in the electronic edition of the *Astrophysical Journal*. A portion is shown here for guidance regarding its form and content.

2.2. *RXTE Data*

The X-ray component of our program consisted of monitoring γ Cas with the *RXTE* satellite using the Proportional Counter Array (PCA), which detects photons in the 2–30 keV energy range. We used the FTOOLS reduction package to complete the pipeline processing of the data and to generate "standard 2″ light curves with a bin time of 16 s.

This program, designated P90001 in the *RXTE* Guest Observer Cycle 9, was designed to monitor this star at the same times our APT system was active during nighttime in Arizona. As a hedge against inclement weather, we asked the *RXTE* project to monitor the satellite during four orbits on each of four nights distributed over several days during a time when γ Cas was situated close to the continuous viewing zone of the satellite. The project was able to meet this request by allocating 8 hr on each of the nights of 2004 November 5, 9, 13, and 14 (UT dates). Our results met the statistics we expected (i.e., they were neither lucky nor unlucky), since it turned out that we obtained overlap with the APT monitoring on two of the four nights. Counting brief interruptions from Earth occultation, South Atlantic Anomaly (SAA) passages, and a high radiation storm, we obtained a total on-target time of 21.3 hr on γ Cas.

During nearly all the PCA observations, three of the five PCU detectors actively integrated on our target. In these cases, count rates given in § 3 are scaled by 5/3 to make them directly comparable with the rates given by Smith et al. (1998a, hereafter SRC98). The *RXTE* PCA is an efficient photon detecting system, and the errors in the net light curve are elevated by only several percent above the combined Poisson errors of the gross and model background fluxes (see also SRC98).

3. RAPID OPTICAL AND X-RAY VARIABILITY

3.1. *Optical Color Variations*

The first step in our analysis of the optical APT data was to determine the mean $\Delta B/\Delta V$ slopes of the variations, which RSH02 showed to be dominated by the optical cycles. We plotted the V against B magnitudes for each of the nine seasons and found that the mean color slope is 0.69. However, we found that these slope values seem to cluster around two values of about 0.63 and 0.73. For example, there are no season-averaged slopes in the range 0.66–0.70. Since the formal significance of each of the seasonal average ratios, including the observational errors is about ± 0.05, these differences are marginally statistically significant to 3 σ for the two seasonal group means. We show an example of these contrasting behaviors for seasons 2000–2001 ("2000") and 2001–2002 ("2001") in Figure 1. Inspection of this plot discloses that the 2001–2002 magnitudes (*squares*) have a steeper slope than the 2000–2001 data (*dots*). The respective slopes for these two seasons are 0.73 and 0.61.

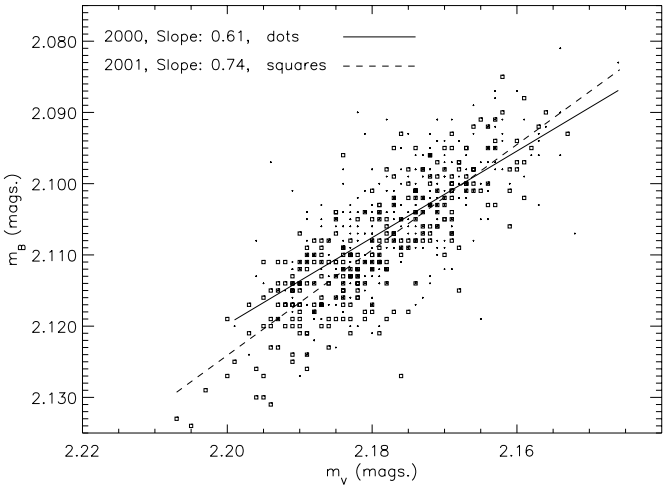

FIG. 1.—The m_V, m_B scatter plot for APT observations of γ Cas during the 2000–2001 and 2001–2002 seasons. The regression line slopes indicated by solid and dashed lines differ from one another at a significance level of 2.4 σ.

The reddish color of these ratios implies that the cyclical flux changes originate in gas cooler than the effective temperature of the Be star. Following RSH02, we suggest that this region is part of the star's decretion disk for two reasons. First, extensive Be disks are well known to contribute to the color of a Be star. No other structure (or star) exists near γ Cas that could be responsible for a 2%–3% variation in the combined optical light. Second, this change is consistent with the color changes observed during the evolution of disks, both in other Be stars and γ Cas itself. If continued accumulation of seasonal averages supports this implied bimodality (four low values, five high), it would likely mean that the variations are caused in different spatial regions of the disk. However, it will take at least a few more years of monitoring to substantiate this speculation.

3.2. *Rapid X-Ray/Optical Variations*

Our attempt to obtain comparisons of simultaneous observations of light and X-ray flux variability was significantly marred by ground or satellite "weather" during each of our four nights of observations in 2004 November. On November 5, we obtained *RXTE* data during a total span of 3 hr, but about one-half of this collection was interrupted by the detectors shutting off during the *RXTE* satellite's passage through the SAA or cloudy weather in Arizona. Our most successful monitoring lasted 7.2 hr on the night of November 9, although it was interrupted by a 2 hr radiation storm. On November 13 the target was monitored over 1.7 hr, of which about 0.6 hr was interrupted by a SAA passage. No APT data were collected due to cloudy weather on November 14. To compare the first three nights of X-ray and optical fluxes, we binned the *RXTE* 16 s data to the APT's time sampling of about 10 minutes and compared these means with any APT observations within 8 minutes of each mean. This gave 4, 24, and 10 paired simultaneous observations for November 5, 9, and 13, respectively. The data for November 5 were insufficient for comparison.

In Figure 2 we depict the simultaneous APT and *RXTE* data for γ Cas on November 9. Because the mean was not well determined, we disregarded the data from November 5 and examined the deviations of the X-ray and optical fluxes from their nightly mean values. As the reader might suspect from visual

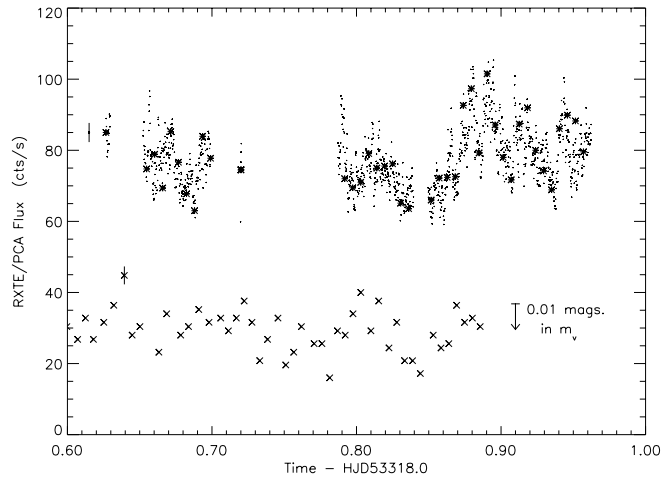

FIG. 2.—Sequence of *RXTE/PCA* fluxes (*dots*) and m_v magnitudes (*crosses*) for γ Cas on 2004 November 9 (HJD 2,453,318). Error bars for the two types of observations are shown. Asterisks represent the X-ray data binned to the same sampling rate as the APT data (*crosses*), or about 10 minutes. The analysis of simultaneous data discussed in the text concerns the paired asterisks-crosses within this range.

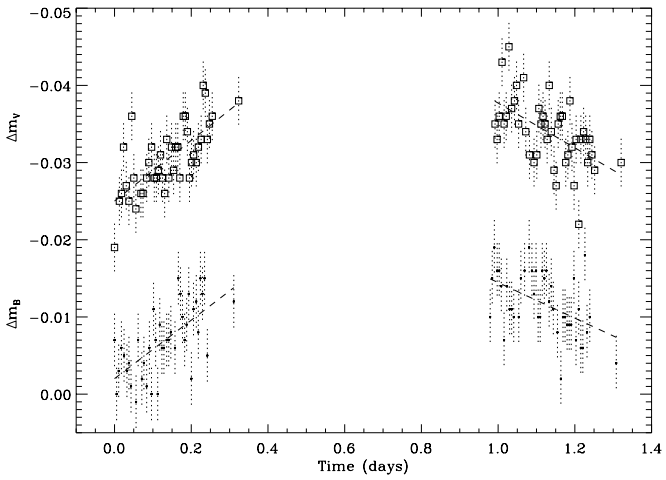

FIG. 3.—Relative *B* and *V* magnitude light curve on the nights of 2003 November 19 and 20 (Julian Dates 2,452,962–2,452,963), shown as squares and dots, respectively (zero points are arbitrary). The dashed curves are linear regression fits to the data.

inspection of Figure 2, the deviations of the X-ray and APT data show no trend at all.[2] Indeed, the correlation coefficients in the X-ray/optical fluctuation scatter diagrams are less than ± 0.1, and these values are changed insignificantly when regressions are run including the effects of errors in the observations. In any case, if we adopt the ratio of X-ray/optical flux variations from RSH02 and the 1997–2004 seasons in § 4 below, namely, $\Delta L_X/\Delta V = 3.0/0.0366 \approx 80 \pm 20$, we find that our scatter plots from November 9 are significantly different from this relation by 8 and 12 σ for the *B* and *V* filters. The same statement can be made to a significance level of 7 σ for the November 13 data. The absence of an optical/X-ray correlation on a rapid (tens of minutes to a few hours) timescale is consistent with the results of SRC98, who found no response in the UV continuum light curve of 1996 March 15, while at the same time *RXTE* observed almost continuous X-ray flaring.

3.3. *Intermediate Timescale Optical/X-Ray Variations*

3.3.1. *Monotonic Trends in Optical Data over Several Hours*

While inspecting the nights of intensive APT monitoring, we found that $\simeq$1% variations with timescales of up to 8 hr are common. Two of these *V* and *B* variations, consisting of rapid light dips or increases, were discussed in RSH02 (see their Fig. 10) and were a motivation for the present study. However, we also found times for which the optical light brightened or dimmed monotonically during an entire 8 hr night. Figure 3 exhibits the *V* and *B* magnitude time series for the nights of 2003 November 19 and 20. For both nights and in both filters the optical light level rises or falls over $\approx$8 hr. The significances of these trends are 6.2 and 4.6 σ (*V* filter) and 5.3 and 3.7 σ (*B* filter).

It is of interest to examine archival X-ray light curves of γ Cas to see whether they exhibit a similar behavior. In particular, we ask what X-ray changes would be implied by these trends if they followed the X-ray/optical correlated flux ratio of $\sim$80? For the data in Figure 3, the optical trends would then translate to X-ray variations of about 50%.

[2] We obtained the same null result when we shifted the X-ray fluxes in time by up to $\pm$14 minutes to account for the contingency that this flux comes from the secondary of the γ Cas system.

To answer the question of whether the X-ray fluxes show an analogous behavior, one can consult the homogeneous *RXTE* light curves published in Figure 6 of RSH02. These data represent the results of six 27 hr monitorings of this star with this instrument during 2000. The light curves show that during 8 hr stretches one can find five similarly sustained changes in the X-ray flux having full amplitudes of 50% or more. These include three increases during visits 1, 2, and 5 of these monitorings and two decreases during visits 2 and 5. These variations comprise five "events" in 112 hr of *RXTE* observation, or one every 22.4 hr.

To compare the frequency of optical and *RXTE* events, we examined the light curves of 13 nights during which the APT monitored γ Cas intensively (37–59 observations) in each bandpass. On these nights we found five nights of sustained increases of $\simeq$0.01 mag (on HJD $-2,450,000 = 52,230$, 52,962, 53,283, 53,319–53,320), two nights of decreases (51,866 and 52,215), and six nights of negligible net change (51,831, 51,834, 52,966–52,967, 53,318, and 53,322). In all cases these trends were significant to at least 3 σ, and the *V* and *B* filter data showed the same trends or constancy. Altogether, the history from the intensive APT observations show seven up/down trends in 104 hr, or an optical rate of one trend event per 14.9 ± 5 hr of monitoring. This is comparable to the X-ray rate of one event per 22.4 ± 10 hr. All told, on any given night the probability of observing a trend is $\sim$7/13. We were apparently unlucky not to catch one of these events in any our four planned all-night monitorings. In any case, it is *plausible*, based on these statistical arguments, that the two behaviors are related to one another and that the $\Delta B/\Delta V$ ratios during a night's observations are close to the ratios found by RSH02 in the correlated long-term cycles. The rhetorical question before us is whether statistical arguments alone based on nonsimultaneous events are a compelling argument for an X-ray/optical correlation.

3.3.2. *How Can the Intermediate-Term X-Ray and Optical Variations Be Understood?*

The short-term events just discussed from the optical and X-ray data are not simultaneous and are too few to demonstrate that they are truly correlated. However, even if they are not correlated, it is not a simple matter to explain how either type of event is produced. The intermediate-timescale optical variations, which have a $\Delta B/\Delta V$ ratio of 0.83 ± 0.07 (e.g., Fig. 3), are difficult to

understand in their own right. The implied red color term suggests that like the cycles, they too are formed in a cool (circumstellar) environment. That they are visible at all implies that they are likely to be formed over volumes considerably larger than the UV-absorbing corotating "clouds" of size $0.2–0.3R_*$. This reasoning suggests that they are most likely to arise in short-lived dense volumes within the disk. If future observations continue to imply that X-ray and optical trend-events occur together with mutually consistent slopes, it may be possible to identify them with local cells that occasionally break away from a generally organized global oscillation of the disk. This would explain why these variations adhere to the X-ray/optical ratio of 80. We note that such occurrences are actually common in astrophysical dynamos, for example, manifesting themselves as "stray" sunspots that appear "out of phase" during solar cycles.

4. THE LONG-TERM CYCLES

4.1. *Continued Correlation of X-Ray and Optical Cycles*

A key result of the RSH02 study was the discovery of a correlation between optical and X-ray cycles of roughly 70 days. This correlation was made possible by a total of eight 27 hr *RXTE* observations that were contemporaneous with the APT observations in 1998 and 2000. In this paper we report on *RXTE* observations that span a total of 9 days. Although this is a much shorter time than a cycle length, the phasing of the new *RXTE* data near the maximum of the optical cycle allows one to predict an X-ray flux at the peak of its cycle and to compare it with the observations. Moreover, our range of 9 days over which the *RXTE* observations were made in 2004 November is large enough to compare with the *slope* of the predicted X-ray variation inferred from the ephemeris for the optical cycle during the 2004–2005 season, as discussed in the next section. The maximum for the sinusoid is taken from an X-ray flux maximum (90 counts s^{-1}), which also corresponds to the optical maximum, according to RSH02. Figure 4 exhibits this comparison. The dots represent the individual X-ray observations. The scatter in these data is mainly fluctuations in the X-ray fluxes caused by flares and changes in the basal flux contribution. The dashed line in this figure is the RSH02 prediction for the maximum of an optical cycle. We emphasize that other than applying the X-ray/optical conversion factor of 80, *no scaling or adjustments have been made in constructing the sinusoidal curve in this figure*. The agreement of the trend represented by the dashed curve to the data represents a confirmation of the correlation of the X-ray and optical cycles found by RSH02.

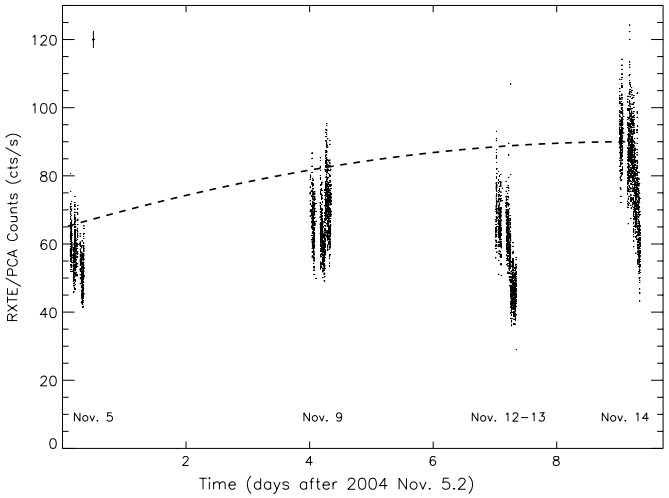

FIG. 4.—*RXTE* PCA light curve for γ Cas for our program. Each dot represents a 16 s integration. The scatter is due to rapid flaring and to slow chaotic undulations; the errors in the observations, shown in the top left, are very small by comparison. Time zero refers to 2004 November 05.0 (i.e., HJD 2,453,314.5). The dashed line is the *predicted* cyclical behavior of the X-ray flux based of the contemporaneous 85 day optical cycle determined by the robotic ATP system located in Arizona. This curve was computed from the X-ray/optical relation over several cycles found by Robinson et al. (2002). *No* time or flux adjustments have been made in its representation.

4.2. *The Optical Cycles*

In this section we consolidate the data for nine seasons of APT observations of the cycles of γ Cas. For each season we have fit the data to a suitably modified sine curve. We started from the results of RSH02 that the mean light level, semiamplitude period may change during a season. In our graphical solutions we have permitted these parameters to float freely, but we left the time of zero phase fixed. We modified the period by introducing a fixed rate of change through a season, that is, by assuming that $\dot{P}$ is a constant. The modified representation becomes

$$m_v = m_0(t) + a(t)\sin\{(2\pi/\dot{P})\ln[1 + (\dot{P}/P_0)t] + \phi_0\}, \quad (1)$$

where $a(t)$ and $m_0(t)$ are linear representations in time. The logarithm in equation (1) supplies higher order terms beyond the first-order expansion term in $\dot{P}$ used by RSH02. This fact explains slight differences we have rederived for the 1999–2000 and 2000–2001 cycles. However, like RSH02, we find that the periods derived for these seasons are too imprecise to link the cycles of these two seasons by a simple linear interpolation. RSH02 also noticed that they were unable to interpolate linearly between the seasonal periods of 65 and 79 days for 1999 and 2000, respectively, without postulating phase changes between these seasons. Likewise, in the current analysis we have found other cases in which a period generated from the data within a season does not fit the extrapolation from the previous season. In some cases these mismatches cannot be easily accommodated by assuming a smoothly increasing or decreasing period between the seasons. Because this may actually be the rule, it is more appropriate to examine the behavior of the cycles within each observing season rather than potentially overlooking interesting physics implied by these anomalies.

Figure 5 shows our best modified sine curve fits to the 1997–2004 cycle data for the V filter. Results for the B filter are virtually the same, except that the amplitudes are slightly smaller. We also note that these data are uncorrected for the small-amplitude, 1.2 day period discussed in the next section. As this paper was being completed, we undertook an analysis of the 2005–2006 data set. However, because we soon discovered that this particular light curve was difficult to interpret even in terms of the increased parametric representation for the earlier cycles, we have not presented the results in our general discussion. The electronic version of Table 1 includes the full data set for readers interested in pursuing the behavior of this season's light curve in detail.

Table 2 gives the corresponding parameters for each season, including the start and end mean magnitudes of our solution for the 1997–2004 seasons. All values are given in days (HJD) and magnitudes. Errors have been computed by investigating the values needed to give just unacceptable fits for each season and taking averages of the results. These errors have meaning only in the context of our models for individual seasons. The reader should note that a negative value for the dimensionless quantity $\dot{P}/P$ corresponds to a lengthening period. The mean full amplitude

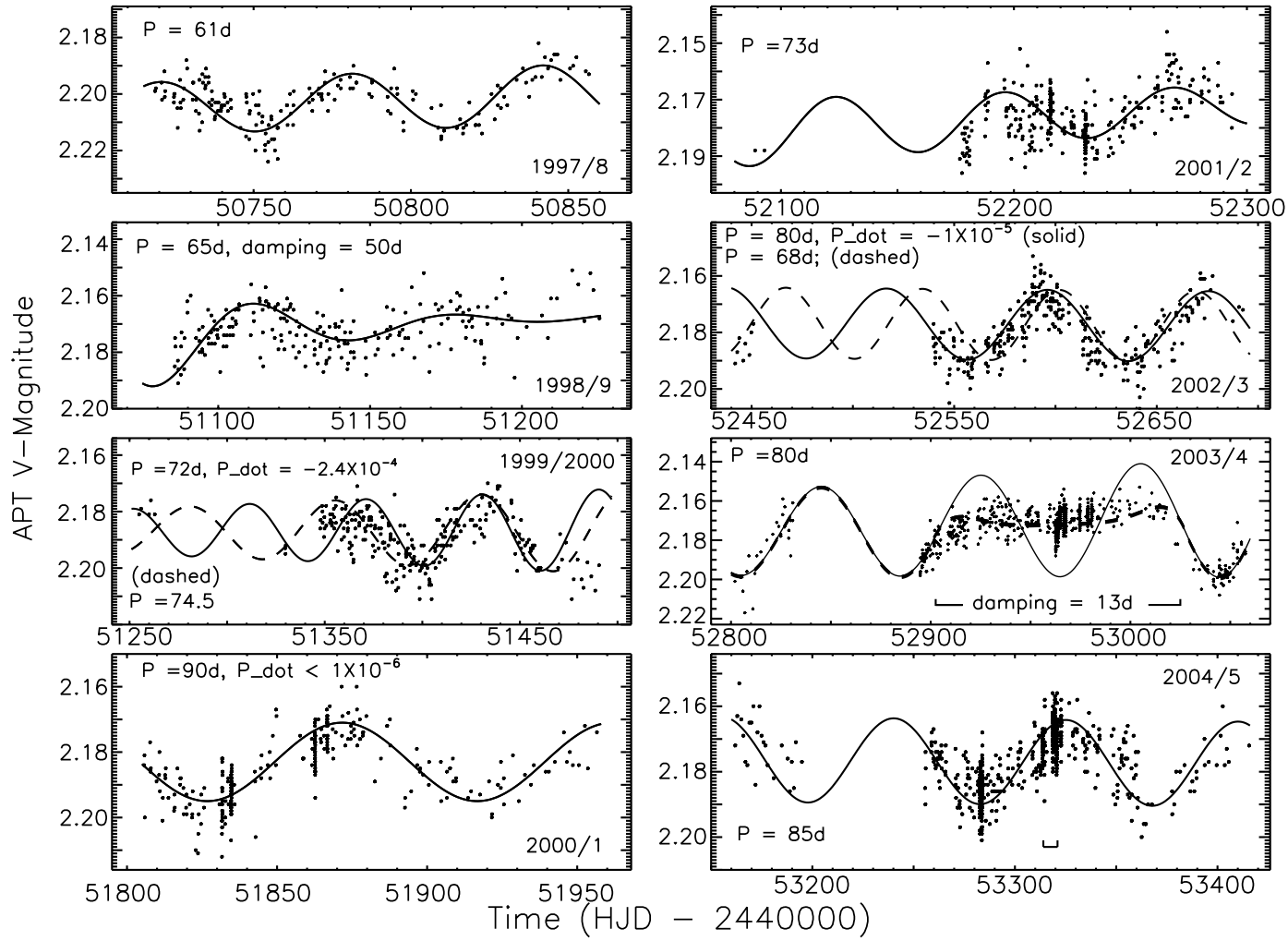

FIG. 5.—Cycles for 1997–2004 seasons. Dashed lines denote alternative (constant period) solutions or an undamped fit (2003–2004). The comb at the bottom of 2004–2005 panel shows the time interval of simultaneous APT-*RXTE* observations. The magnitude scale on each of the figures is the same except for season 2003–2004. As in other representations, the magnitude zero is uncertain for season 1997–1998.

for the cycles in the V filter, computed as twice the sum in quadratures of the two semiamplitudes given in the table, is 0.0366 mag. These amplitudes and the X-ray amplitude in Figure 4 account for the $\Delta L_X/\Delta V$ of 80 we have adopted. In constructing these fits we noticed the following departures from constant-amplitude fits:

1. During at least two seasons, 1998–1999 and 2003–2004, the cycles are exponentially damped. Their damping constants are 50 days and 13 days, respectively. Surprisingly, the 2003–2004 light curve grows again exponentially to an even larger amplitude than it had at the beginning of the season. Both the damping and growth rates are 13 days. It is further remarkable that little or no phase change occurs during this transition.

2. The damping behavior could mislead one to interpret the lengths of some of the cycles to be about double their true values. Our discovery that the cycles can damp out, particularly near an extremum, can sometimes require different values for the cycle lengths than appreciated by RSH02. For example, their

TABLE 2

CYCLE FIT PARAMETERS TO TWO SINUSOIDS

Year	P_0	$\dot{P}/P$	a_1	a_2	$\langle m_v(\text{start})\rangle$	$\langle m_v(\text{end})\rangle$	t_0 - HJD 2,400,000
1997–1998.....	61	0.0	0.009	0.011	2.165	2.160	50750.2
1998–1999.....	65	0.0	0.020	~0	2.134	2.170	51145.7
1999–2000.....	72	-2.4×10^{-4}	0.008	0.0015	2.147	2.147	51311.2
2000–2001.....	91	0.0	0.012	0.0012	2.143	2.143	51825.0
2001–2002.....	73	1.5×10^{-5}	0.012	0.007	2.142	2.132	52123.3
2002–2003.....	80	-1.0×10^{-5}	0.0125	0.0125	2.1365	2.138	52521.8
2003.....	80	0.0	0.021	0.031	2.137	2.128	52805.5
2004–2005.....	85	0.0	0.013	0.013	2.1362	2.1377	53197.5

NOTE.—Errors: $\delta P = \pm 2$ days, fractional $\dot{P}/P = \pm 20\%$, a_1, $a_2 = \pm 0.001$ mag, $\langle m_v\rangle = \pm 0.002$ mag, $t_0 = \pm 3$ days.

assignment of 55 days for the period of the 1998–1999 was the unforeseen result of not appreciating the damping behavior.

3. It is also likely (see Fig. 5) that the 1999–2000 season is affected by a similar, although longer, growth in amplitude as compared to the previous season. RSH02 found that cycle amplitudes can change from one year to the next. We see now that the timescale over which this occurs can vary significantly.

4. Changes in the period can occur over intervals shorter than the period itself (RSH02's "change in phase"). Although in Figure 5 we have represented the 1999–2000 cycles season by both a simple (but growing in amplitude) sine wave and one with an increasing period (*dashed line*), it is also possible to fit the data with a sine curve in which the phase seems to lag by 20–30 days at the time of minimum of the second cycle.

5. The periods can change in more complex ways than are represented by a single $\dot{P}$ term in equation (1). For example, the data in the 2002–2003 season can be fit adequately only by allowing the "period" to shorten and then lengthen during this interval. Thus, neither the dashed- nor the solid-line representation, denoting a constant period or constant $\dot{P}$, respectively, can represent the obvious change in intervals between the three minima of this season.

6. The mean magnitudes change slowly from season to season, exhibiting values, for example, of 2.171 and 2.188 mag for 1998–1999 and 1999–2000, respectively. These changes, together with growth/dampings of cycles, can produce ambiguities in the interpretation of the cycle length and even the analysis of signal in other frequency ranges. For example, we are unable to analyze the variations during the 2005–2006 season yet because we do not know how to model the change in the mean magnitude over this season. The light curve at this time appears first to undergo part a long cycle, then brighten, and finally develop a robust, short cycle of $\approx$50 days. This behavior falls well outside even the expanded parametric representation of the cycles in this paper.

An examination of these fitting parameters indicates no correlation among them, for example, of amplitude with time, nor are they correlated with the yearly $\Delta B/\Delta V$ values or with the much longer V/R Hα emission data given by Miroschnichenko et al. (2002). It is much too early to be able to associate cycle attributes with one another.

Finally, we point out that RSH02 found the correlated optical/X-ray cycles from the 1999 and 2000 cycles in this plot. In addition, we note that the slightly low X-ray flux recorded during November 1998 (Robinson & Smith 2000) corresponds to the weak secondary minimum of the 1998–1999 optical cycle shown in Figure 5.

4.3. *The Viability of the Dynamo Model*

The suggestion in RSH02 that the correlated variations in X-rays and optical emission are ultimately due to dynamo cycles in the decretion disk remains an attractive hypothesis. However, there are significant differences between the dynamics of this system and any of the current numerical simulations of disk dynamos in the literature. The bulk of the decretion disk mass, and most of its optical emission, comes from the inner regions of the disk, where the magnetic field of the star may be strong enough to enforce corotation out to at least $\sim 1R_*$ above the star's surface (RSH02). If one takes the characteristic density of the disk to be 10^{12}–10^{13} cm^{-3}, then the strength of the stellar magnetic field in pressure equilibrium with respect to the bulk kinetic (i.e., orbital) energy should be a few hundred gauss near the corotation radius. This is consistent with a typical magnetic field strength at the stellar surface of more than 10^4 G (see § 5.4) in a highly disordered field. On the other hand, a disk dynamo will be driven by the magnetorotational instability (MRI), which will saturate at a magnetic energy density less than the thermal pressure in the disk. This density corresponds to a magnetic field strength of $\sim$10 G. Numerical simulations (for a review, see Balbus & Hawley 1998) suggest that magnetic fields may fail to reach this limit by an order of magnitude, depending on the orientation of the field in the disk. Apparently, in the absence of mitigating factors, we might expect the stellar magnetic field to dominate over any plausible MRI dynamo field by a factor of roughly 100. Such a strong externally driven field would act to suppress the local MRI instability, although the global stability of the system is uncertain (Spruit et al. 1995; Stehle & Spruit 2001). We conclude that unless arguments can be advanced that the stellar field is somehow excluded from the disk, for example, by the stellar wind (see, e.g., ud-Doula & Owocki 2002), its influence on the disk field could quench the MRI dynamo mechanism.

Despite this problem, it is in any case possible that long timescale variations in γ Cas are the result of disk instabilities. One possibility is that the dynamo mechanism may have little to do with the MRI dynamo. Instead, the instabilities may be a heretofore uncontemplated result of nonlocal interactions between the disk and the star. In either case it is clear that the available simulations of the disk dynamos are an unreliable guide to the dynamics of this system.

5. DISCOVERY OF A 1.2 DAY PERIODICITY

5.1. *Observational Characteristics of a 1.2 day Periodicity*

The initial motivation to monitor γ Cas with the APT was to search for a signature of the rotational period. For a broad-lined, early B-type star on the main sequence, this period should be near 1 day. To search for such a period, we analyzed the nine individual seasons of our γ Cas observations with the method of Vaníček (1971). This procedure is based on least-squares fitting of sinusoids. Henry et al. (2001 and references therein) describe how this method allows us to locate and fix individual frequencies in succession to determine all of the multiple frequency components present in a data set. The Vaníček method differs from prewhitening for a given frequency before searching for the next by the investigator's fixing only the given frequency, and not its amplitude, phase, or mean light level, before computing a new power spectrum. The new frequency search is carried out while simultaneously fitting a single new mean brightness level along with the amplitudes and phases of all frequencies introduced as fixed parameters. In the resulting least-squares spectra, we plot the fractional reduction of the variance (reduction factor) versus trial frequency. This method holds an advantage over prewhitening, especially in the low-frequency domain, where mean light levels, amplitudes, and phases might be poorly determined. Thus, it avoids perpetuating systematic errors in these parameters in successive searches for additional frequencies.

We applied this strategy to each of the nine seasons of our γ Cas photometry by searching the frequency range 0.001 to 2.5 day^{-1}, corresponding to a period range of 0.4 to 1000 days. In each season, for both the V and B data sets, we found evidence for a weak frequency near 0.8225 day^{-1}, or approximately 1.215 days, after fixing three low frequencies arising from the cycles discussed in § 4. Because of the changing nature of the stronger cycles and the difference in the cadence of the observations from season to season (see § 2.1), the robustness of the 1.215 day signal we found varied significantly from year to year.

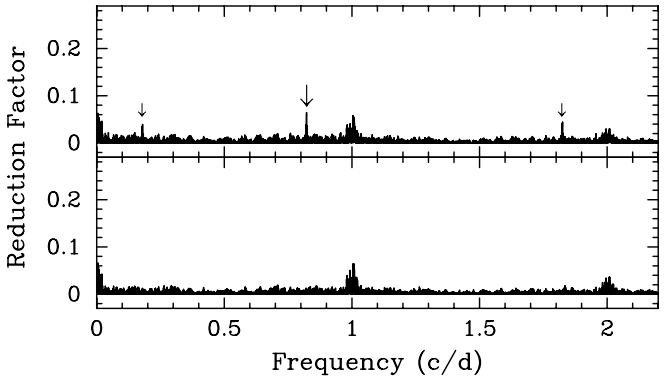

FIG. 6.—*Top:* Power spectrum of the season 2 through 8 *V* observations after fixing the low frequencies 0.01225, 0.00838, and 0.00321 day^{-1}. The ordinate is the fractional reduction of the variance. The strongest remaining frequency, marked with the large arrow, is 0.82250 ± 0.00001 day^{-1}, corresponding to a period of 1.21580 ± 0.00002 days. The smaller arrows mark the ±1 day aliases of the ±0.82250 day^{-1} frequency. *Bottom:* Power spectrum showing the results of fixing the three low frequencies *and* the 0.82250 day^{-1} frequency. There are no other frequencies in this range that appear significantly above the noise level, except for the 1 day aliases of remaining low-frequency variation.

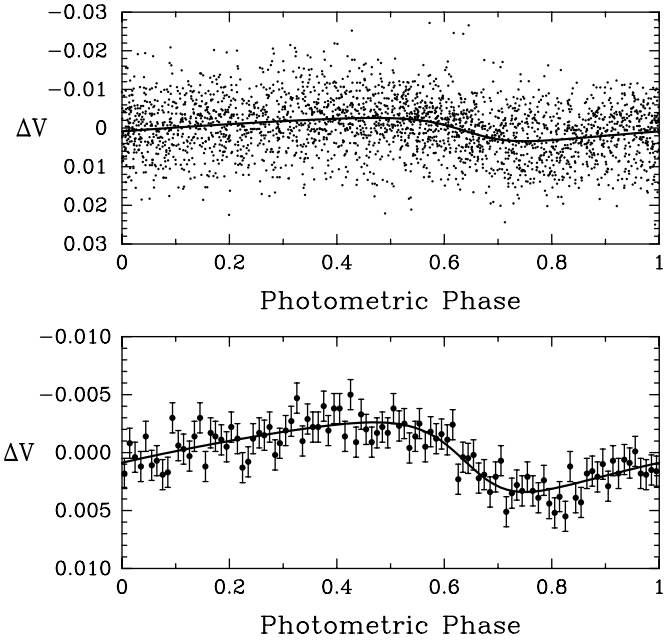

FIG. 7.—*Top:* Season 2–9 photometric *V* observations phased with the 1.21851 day period and the arbitrary epoch HD 2,450,000. The data have been prewhitened to remove the low frequencies given in the text; the mean is also removed. The solid line is the fit for a Lehmann-Filhes function (eq. [2]). *Bottom:* Data from the top panel averaged into 100 phase bins and plotted with an expanded scale for the *y*-axis. Error bars give the standard deviations of the mean for each bin. The solid curve is the same one in the top panel. The binned data show good conformance to the now more discernible mean curve.

As an additional check on the presence of the 1.215 day period, we repeated our period analysis on the combined seasons 2–8 data sets. We omitted season 1 from this analysis because of the undetermined offset of those observations (§ 2.1). We also omitted season 9 (2005–2006) for a similar reason, namely, that a difficult-to-model brightening of the star during this season produced several spurious low-frequencies in our raw periodogram and large errors in a final solution. For the analysis of seasons 2–8, the 0.8225 day^{-1} frequency was visible in the power spectrum, suggesting the possibility that the 1.215 day period remains coherent in phase throughout our monitoring program. The top panel of Figure 6 shows shows the resulting power spectrum of the seasons 2–8 *V*-filter observations after fixing the low frequencies 0.01225, 0.00838, and 0.00321 day^{-1}. The strongest remaining frequency, marked with the large arrow, is 0.82250 ± 0.00001 day^{-1}. This corresponds to a period of 1.21580 ± 0.00002 days. The smaller arrows mark the ±1 day aliases of the 0.82250 day^{-1} frequency. The small clusters of frequencies at 1 and 2 day^{-1} are the 1 day aliases of the residual low-frequency variations visible at the extreme left of the top panel that have not been fixed in this analysis. The bottom panel of Figure 6 shows the results of fixing the previous three low frequencies *and* the 0.82250 day^{-1} frequency. There are no other frequencies in this range that appear significantly above the noise level. We repeated this analysis with the season 2–8 *B*-filter observations with nearly identical results. After fixing three low frequencies at 0.00837, 0.01222, and 0.00383 day^{-1} in the *B* data, the strongest remaining frequency was 0.82249 ± 0.00001 day^{-1}, corresponding to a period of 1.21582 ± 0.00002 days. Thus, the mean period from the *V* and *B* data sets is 1.21581 ± 0.00002 days. An additional search for higher frequencies out to 30 day^{-1} was negative.

The top panel of Figure 7 plots the variations of all the *V* observations from seasons 2–8 after prewhitening for the four low frequencies mentioned in the above paragraph and phased with the 1.21581 day period and the arbitrary epoch HJD 2,450,000. A similar plot for the *B* observations is essentially identical. The peak-to-peak amplitudes of the 1.21581 day period in the *V* and *B* passbands, based on least-squares sine fits of the non-prewhitened original data sets, were 0.0053 ± 0.0004 and 0.0055 ± 0.0004 mag, respectively. Thus, the amplitudes are identical within their uncertainties.

Inspection of Figure 7 reveals that the waveform is highly nonsinusoidal. Indeed, the maximum occurs at phase ∼0.49, while the minimum is visible at about 0.71. Such an asymmetric waveform is unusual in astrophysical processes that generate a single oscillation. This property suggested that the waveform could be fit analytically by a Lehmann-Filhes solution, in the manner of fitting radial velocity solutions of a binary star. Then the functional form of the single-wave curve is given by

$$m = K \cos(\phi + \omega) + e \cos(\omega). \quad (2)$$

Here *m* represents the apparent magnitude rather than a radial velocity, and *K*, ϕ, *e*, and ω can be thought of as analogs of the orbital parameters velocity semiamplitude, phase, eccentricity, and longitude of periastron. The latter quantity is an arbitrary phase zero point similar to our arbitrary photometric epoch of JD 2,450,000. We verified the aptness of this functional fit by binning the phase curves into 100 bins (0.01 cycles) and overplotting the 0.01 cycle means with the solution. This is shown in the bottom panel of Figure 7. No systematic departures of the binned data could be discerned with respect to the solution in either data set, further suggesting that the 1.21581 day period is coherent throughout our data set. For the *B* filter our solution is $K = 0.00300 \pm .00013$ mag, $e = 0.333 \pm 0.049$, and $\omega = 280.3 \pm 9.9$, while for the *V* filter it is $K = 0.00302 \pm .00013$ mag, $e = 0.372 \pm 0.052$, and $\omega = 289.6 \pm 9.7$. Since this waveform is to be preferred over the sinusoidal representation, the derived *K*-values should be regarded as the true semiamplitudes of the variation. We also note that the K_B/K_V ratio is near unity, or formally 1.00 ± 0.06. Since the quoted errors do not reflect the

TABLE 3
INDEPENDENT SINUSOIDAL FITS TO 1.2 DAY PERIODS FOR YEARLY γ CASSIOPEIA OBSERVATIONS

Year (1)	P = 1.21581 Peak-to-Peak Amplitude (mag) (2)	P = 1.21581 Phase of Minimum (phase units) (3)	Control: P = 1.1976 Peak-to-Peak Amplitude (mag) (4)	Control P = 1.1976 Phase of Minimum (phase units) (5)
1998–1999	0.0066 ± 0.0015	0.921 ± 0.036	0.0085 ± 0.0015	0.242 ± 0.028
1999–2000	0.0066 ± 0.0015	0.818 ± 0.036	0.0109 ± 0.0015	0.256 ± 0.022
2000–2001	0.0028 ± 0.0018	0.775 ± 0.091	0.0061 ± 0.0017	0.170 ± 0.042
2001–2002	0.0095 ± 0.0014	0.848 ± 0.023	0.0071 ± 0.0014	0.374 ± 0.030
2002–2003	0.0053 ± 0.0017	0.816 ± 0.048	0.0075 ± 0.0016	0.211 ± 0.035
2003–2004	0.0040 ± 0.0012	0.783 ± 0.044	0.0039 ± 0.0012	0.425 ± 0.045
2004–2005	0.0112 ± 0.0009	0.985 ± 0.013	0.0051 ± 0.0010	0.235 ± 0.030
2005–2006	0.0032 ± 0.0011	0.049 ± 0.055	0.0046 ± 0.0012	0.261 ± 0.040
σ	0.0030	0.074	0.0025	0.089

ambiguity of the "correct" filtering of long periods, we believe our quoted errors should be increased by 50%–100%. We can check this result spectroscopically by comparing the strengths of lines from prominent UV multiplets of C II, Si III, Si IV, and C IV in *IUE* SWP camera echellograms obtained during "bright-" and "faint-star" times, according to equation (2), during the 1982 and 1996 campaigns on γ Cas. These spectra show no significant variations of the line strengths that would be expected due to thermal variations on the star's surface and are therefore consistent with a near-unity ratio of K_B/K_V. The same comments apply to the absence of phased variations of the optical components of the Si IV doublet discussed by SRH98.

As a final check on the long-term amplitude and phase coherency of the 1.21581 day period, we fit least-squares sinusoids at that period to the non-prewhitened data in the individual observing seasons 2–9 independently. Table 3 lists the resulting peak-to-peak amplitudes in V and phases of minimum for the eight observing seasons in columns (2) and (3), respectively, along with their individual formal errors. Notice that standard deviations of the amplitudes and phases are 0.0030 mag and 0.074 phase units, respectively, both significantly larger than the typical formal errors. This could suggest conceivably that there are season-to-season variations in amplitude and phase and thus some degree of noncoherency in the 1.21581 day period. However, as noted earlier, the natures of the cycles and the cadences of the observations are significantly different from season to season. This situation could result in systematic errors in the amplitudes and phases that would render the formal errors too small. To test this hypothesis, we removed (prewhitened) the 1.21581 day period from the seasons 2–9 V light curves and added a similar but randomly chosen 1.1976 day coherent variation with the same amplitude as the 1.21581 day period. We then repeated the sine curve fits for the individual seasons using the artificial 1.1976 day period. The results are given in columns (4) and (5) of Table 3. The standard deviations of the amplitudes and phases of the artificial 1.1976 day period are 0.0025 mag and 0.089 phase units, similar to our results with the 1.21581 day period and also larger than the typical formal errors. Therefore, this result is consistent with the amplitude and phase stability of the 1.21581 day period throughout our complete data set. This addresses the disparity between the "sigma" in the table and the formal photometric errors.

5.2. *The Rotational Nature of the 1.2 Day Period*

Three possible explanations present themselves for a coherent 1.2 day period in an early B star: rotation, ellipsoidal variation, and (nonradial) pulsation. Among these, rotation is by far the most likely mechanism, primarily because it is well within the narrow range of rotational periods suggested for this star. The rotational period can be determined by knowing the rotational velocity, radius, and rotational obliquity, i. Recent values of the rotational velocity are 400 and 432 km s^{-1} (Harmanec 2002; Zorec et al. 2005), the mass and log gravity are 15.2 ± 0.9 $M_\odot$ and 3.80, respectively. As already mentioned, values of i ranging from 46° to 60° have been determined from interferometry. This range of parameters gives an expected range for the rotational period of 1.08–1.41 days. The mean of these is 1.245 days, which is close to the 1.21581 period from our APT photometry. However, before accepting rotation as the driver of this variation, we consider the competing explanations.

One may dismiss readily the possibility that the 1.2 day period arises from an ellipsoidal variation of the Be star in a 2.4 day orbit. Such a variation could only arise in a binary with comparable component masses in a close system. It would produce a radial velocity variation, 2K, of tens of kilometers per second, which would have been easily observed, e.g., in the data of Harmanec et al. (2000) and Miroschnichenko et al. (2002). In addition, a 2.4 day system would be tidally locked for a main-sequence B star. The photospheric line profiles are much too broadened to arise on a star having this long a rotational period.

Arguments against nonradial pulsations are also strong, but not as clear cut. Empirically, we know that NRPs in B stars are often multiperiodic. Yet secondary periods are not in evidence in our periodogram.

An important theoretical argument is that the NRP periods are *expected* to decrease with $T_{\rm eff}$ in B stars because their values should be of the order of the thermal timescale in the Z-bump driving zone where the pulsations are excited (e.g., Pamyatnykh 1999). Since these timescales for ~B0.5 IV stars are only several hours, they are incompatible with the 1.2 day period. Observationally, no other early B or late O stars are known with periods near a day. Indeed, the best examples of stars in this domain, such as ζ Oph and HD 93521 (Reid et al. 1993; Howarth & Reid 1993), have periods of only several hours. A final argument against NRP concerns the observed waveform. Given the small observed amplitude, if the 1.2 day signal were due to NRP, the oscillation would have to be small and subsonic. In this circumstance there is no reason to expect that its waveform should depart from a sinusoid. Yet, according to our canvassing of the NRP literature, the available light and line profile flux curves of B variables, even with much larger amplitudes, exhibit waveforms that are nearly sinusoidal. This is very unlike the morphology shown in Figure 7.

5.3. *Previous Claims of a Rotational Period*

The 1.2 day period is at variance with several claims in the literature of a rotational period for γ Cas. These include claims by Harmanec (1999) of a spectroscopic period. More challenging are reports by Marchenko et al. (1998) and Harmanec et al. (2000) of a total of three periods in the range of 1.04–1.64 days in the *Hipparcos* (Perryman 1997) light curve. In addition, SRC98 and SRH98 found a period of 1.123 days from *RXTE* and *IUE* fluxes. We discuss each of these as follows.

Harmanec's (1999) estimate of 1.16 days, close to our own, was based on the assumption that the acceleration of MSFs in optical line profiles is due to fixed disturbances on the star's surface. This value, unlike ours, is subject to uncertainties in the estimated inclination and radius of the star. Moreover, it is especially sensitive to the assumed distance above the star's surface of the clouds that are responsible for the placement of the MSF disturbances on the star's surface. His result can be expected to be imprecise, but rather close to our own, as indeed it is.

We have repeated the analysis by Marchenko et al. (1998) and Harmanec et al. (2000) of the *Hipparcos* light curve. We agree with the latter authors that the *best candidate period* in the *Hipparcos* light curve is 1.487 days, However, when the data set is broken into two and three segments, this signal is found to be confined to the middle segment and therefore cannot be described as a coherent period. From our examination of this light curve, we conclude that no coherent periods near 1 day can be reliably found. The principal problem is that the *Hipparcos* data are too sparse and poorly sampled to resolve the long-term, low-amplitude (3%) 50–91 day irregular cycles in γ Cas. It appears that the short periods derived by these authors are likely to be aliases of these long cycles, as discovered in our own analysis and recounted above. Our conclusion is confirmed by our experience with comparisons of other extended APT data sets and corresponding *Hipparcos* light curves. For example, Henry et al. (2000) have used comparable quality APT data for a large sample of stars, many of which were found to be variable, with full amplitudes as low as 0.6%. These same stars were also observed by *Hipparcos*. Variability was generally not found in the latter light curves when the amplitudes were less than 3%. Similarly, Henry & Fekel (2002a, 2002b) used APT data to discover periods in six new γ Dor and five δ Scu variables, respectively. Only two of these stars showed indications of variability in the *Hipparcos* data. However, because two-channel photometers were used, this probably slightly overstates the relative APT advantage.

The 1.2 day period likewise contradicts the SRH98 claim of a period near 1.12 days. This claim was based on bootstrapping from an initial rough (and nonunique) estimate obtained from an analysis of UV continuum dips in a 1.2 day time series of *IUE* observations. SRC98 supposed that these dips correspond to repeating X-ray maxima over many rotations. Based on their search for a rotational marker in a series of 6 1.1 day *RXTE* observations, RSH02 concluded that such markers may disappear within a week, or about six rotation cycles. Indeed, this discovery undermined a key assumption made in deriving the SRH98 period.

5.4. *The Origin of the Periodicity*

Explanations for the origin of this period are not yet well constrained, but there is perhaps enough information to point us in the right direction. Possible locations of the origin of the rotational signature are the surface of the star and a corotating structure just above the stellar surface. The sawtooth waveform presents a difficulty for either case. The circumstellar explanation at first seems attractive because we know that such clouds exist. The absence of a noticeable color variation means that the continuum-emitting clouds would have to have the photospheric temperature and thus be close to the star. In this picture, the fact that the light level falls below the maximum during most of the cycle would mean that emitting clouds are distributed over a range of stellar longitudes and are occulted as they corotate behind the star. This requirement for proximity to the surface forces the circumstellar explanation to posit the existence of many small dense sources corotating over points on the surface with a range of longitudes. These sources would also have to be optically thick in the continuum, and this requires a column density of at least 10^{25} cm^{-2}. This requirement exceeds by 2 or 3 orders of magnitude the thick component of a two-density model of small circumstellar clouds discussed by Smith & Robinson (1999), based on their analysis of the variable Si IV and S IV line absorptions. While this is not impossible, there is no support for continuum reemission from the cloud properties, for example, from the flatness of the 1996 March GHRS light curve between its obvious dips. These arguments cast doubt on a circumstellar origin for the variations in the optical light curve.

The interpretation we strongly favor is one in which a structure is firmly rooted on the star's surface. To date, we are aware of only one other early-to-mid B-type star, HD 37776, that exhibits rotational modulations (period = 1.538675 days; Adelman 1997) in unpolarized optical-continuum light.[3] This star is special even among Bp variables because of its very strong dipolar field strength (60 kG). The dipole coexists with a quadrupolar component that is nearly antialigned with the primary dipole (Thompson & Landstreet 1985; Khokhlova et al. 2000). The ensemble produces a double-wave light curve. In the visible/red bandpasses the presence of the secondary flux bump is suppressed, with the result that the light curve takes on a quasi-sawtooth waveform (Mikulasek et al. 2006). The star has a heterogeneous surface distribution of the metals (Khokhlova et al. 2000). According to Krticka et al. (2006), a heavy metal patch is the best explanation for the variations in this curve curve.

The example of HD 37776 suggests that large and multipolar magnetic fields on an early-type B star can produce its observed photometric variations over the rotational period. The amplitude of the visible wavelength light curve is about 3.3 times larger than the variations we have reported for γ Cas. A simplistic scaling of the photometric amplitude ratio of HD 37776 with respect to γ Cas would likely lead to an overestimate of the latter's mean surface field strength, particularly if the magnetic topology is as complicated (or more so) as what has been found for HD 37776.

From the foregoing, we believe the best explanation for the monochromatic variations of γ Cas is that they are produced by an undiscovered strong multipolar field rooted on magnetic poles that are distributed over a range of stellar longitudes. The requirement that the fields should be multipolar and distributed across the surface is supported by the broad distribution of X-ray active maxima occurring over several 27 hr long X-ray monitoring campaigns (essentially the rotational period) of γ Cas

[3] By this statement we are excepting the case of the B2p star σ Ori E, which also exhibits continuum light variations (Hesser et al. 1977). The difference is that its photometric variations are the result of absorption from an intervening corotating cloud (Smith & Groote 2001). In contrast, the photometric variations in HD 37776 are well correlated with strengths of spectral lines, also arising from high excitation potentials, e.g., by Khokhlova et al. (2000), and these cannot arise in an unheated circumstellar cloud.

(e.g., RSH02). Indeed, the instances of high X-ray activity are so numerous that it is possible only to discover *inactivity* markers by cross-correlating reciprocal X-ray flux curves (Robinson & Smith 2002; RSH02). Finally, the absence of a single dominant dipolar field is suggested by the lack of evidence of a magnetically focused wind, i.e., modulated low-velocity emissions and absorptions of UV resonance lines (e.g., Shore & Brown 1990). In contrast, these variations are the rule among well-observed magnetic Bp stars.

6. CONCLUSIONS

However well studied, γ Cas has become a prototypical astronomical onion, with each new discovery raising many more questions than answers about the interaction of complex processes in hot unevolved stars. In broad strokes, we can summarize the phenomenology relating to the complicated circumstellar environment by the following description.

A number of recent studies of γ Cas, including the simultaneous *RXTE*-GHRS campaign of 1996, have shown that in addition to the continuum flux, the strengths of a number of UV absorption lines are strongly correlated/anticorrelated with X-ray flux. Altogether, there are at least three systems of circumstellar debris: the (mainly) Keplerian orbiting disk, the corotating clouds of various temperatures (visible in the UV continua or in the UV and optical as MSFs), and redshifted blobs moving at least roughly toward the star. Thus, there is no need to invoke an association of any of the UV and the X-ray activities with the secondary star of the γ Cas binary system. Indeed, the variable ultraviolet diagnostics we found can be expected to be associated with the wind or disk of the Be star, and the X-ray fluxes are in turn correlated with them (Smith & Robinson 1999; Robinson & Smith 2000).

The evidence for a correlation between X-ray and optical cycles continues to accumulate, as in our Figure 4. This seems to suggest that the X-ray production is ultimately tied to properties of a magnetized decretion disk. This argument, along with a non-correlation of epochal X-ray fluxes with respect to the 204 day binary period, led RSH02 to suggest that a mechanism in the disk controls the conditions for hard X-ray production. However, this does not mean that this flux is necessarily emitted in this structure. In fact, the rapid evolution of flares is consistent only with densities of $\geq 10^{14}$ cm^3. This fact led SRC98 to place the flare centers on the surface of the star. The data used in this study is adequate to show that flare aggregates cannot trigger a response at visible wavelengths. SRC98 came to a similar conclusion based on uncorrelated X-ray and ultraviolet continuum fluxes.

A major unresolved issue in our understanding of the correlated X-ray and optical cycles is the possible role of a decretion disk dynamo. If the star's magnetic field intersects the stellar disk, it can be expected to quench an MRI disk dynamo. Perhaps the wind's outward flow prevents the field from crossing the disk plane. According to the geometry of strong stellar winds in magnetic stars, this seems likely to some extent (see Smith & Fullerton 2005; Gagné et al. 2005). At some distances from the star, the wind finally dominates the field and opens outwards toward infinity. Thus, the flow and the field lines no longer penetrate the disk efficiently. Under these circumstances it is conceivable that a dynamo can survive. The intermediate-timescale variations are equally puzzling. Are they evidence for spatially local structures that decouple from an otherwise interconnected magnetosphere/decretion disk system? Or, despite the similarity of their X-ray/optical scaling with the scaling of the long cycles, is the optical flux emitted from somewhere else, such as individual plasma clouds in the magnetosphere?

The most important result of this paper is the discovery of a coherent 1.2 day periodicity in both the B and V filters. The determination of a coherent period clearly moves the production of the X-rays one step closer to the intrinsic properties of the Be star. Like the larger optical variations of the multiorder magnetic B2p star HD 37776, the modulation in the γ Cas light curve has no accompanying $B - V$ color term. Our linking the γ Cas and HD 37776 variations together implies that γ Cas may yet turn out to be chemically peculiar and therefore a member of the Bp class, albeit one even more complex than other members. However, helium is thought to remain closely coupled to hydrogen particles in the winds of hot stars (e.g., Hunger & Groote 1999). Because it is not yet clear whether a mechanism exists to segregate and distribute helium atoms over a star as hot as γ Cas, it may be productive to undertake a search for helium line strength modulations around the 1.2 day period. Such a test, e.g., of He I λ4471 (which appears wholly in absorption), would provide an important means by which to establish whether helium-rich patches associated with the early Bp star can be found in stars hotter than the canonical hot boundary (type B2) of this class.

It is likely that the B0.5–B1 IV star HD 110432 is a new member of the γ Cas "class" (Smith & Balona 2006). In addition to this star, Motch et al. (2006) and Lopes de Oliveira et al. (2006) have suggested the addition of four new members to the group. According to our picture, a γ Cas star requires a dense disk, magnetic field (probably complex), and a rapid rotation. The rapid rotation is necessary to ensure the production of magnetic stresses between the star and the inner region of the Be disk where the rotation law transitions from corotation to Keplerian. The high-order field is an additional (empirical) requirement, based on the absence of rotationally modulated UV resonance lines and Hα emission. These periodic emissions/absorptions over a cycle have proved to be reliable spectroscopic hallmarks of dipolar magnetic Bp stars. The requirement of rapid rotation and a magnetic field may also mean that γ Cas stars exist near the end of their main-sequence evolution stage. This speculation emerges from growing evidence that magnetic fields and CNO-processing products (including He-enhancement) are correlated in evolved stars (Neiner et al. 2003; Lyubimkov et al. 2004; Huang & Gies 2006). If additional abundance determinations of evolved stars confirm this initial trend, γ Cas analogs could be absent in very young clusters because not enough time has elapsed to bring their fields to the surface.

We thank Lou Boyd for his continuing support of the automatic telescopes at Fairborn Observatory and Frank Fekel for providing the Lehmann-Filhes fit to the phase curve in Figure 7. We also want thank David Bohlender for pointing out the relevance of HD 37776 to this paper. It is also a pleasure to thank both Steve Cranmer and an anonymous referee for suggestions that improved this paper. This work was supported by NASA grant NNG05GB60C to the Catholic University of America and by NASA grant NCC5-511 and NSF grant HRD 97-06268 to Tennessee State University.

REFERENCES

Adelman, S. J. 1997, A&AS, 125, 65
Balbus, S., & Hawley, J. F. 1991, ApJ, 376, 214
———. 1998, Rev. Mod. Phys., 70, 1
Berio, P., & Stée, Ph. 1999, A&A, 345, 203
Breger, M. 1974, ApJ, 188, 53
Gagné, M., et al. 2005, ApJ, 628, 986
Harmanec, P. 1999, A&A, 341, 867
———. 2002, in ASP Conf. Ser. 279, Exotic Stars as Challenges to Evolution, ed. C. A. Tout & W. van Hamme (San Francisco: ASP), 221
Harmanec, P., et al. 2000, A&A, 364, 85
Henry, G. W. 1995a, in ASP Conf. Ser. 79, Robotic Telescopes: Current Capabilities, Present Developments, and Future Prospects for Automated Astronomy, ed. G. W. Henry & J. A. Eaton (San Francisco: ASP), 37
———. 1995b, in ASP Conf. Ser. 79, Robotic Telescopes: Current Capabilities, Present Developments, and Future Prospects for Automated Astronomy, ed. G. W. Henry & J. A. Eaton (San Francisco: ASP), 44
Henry, G. W., & Fekel, F. C. 2002a, PASP, 114, 988
———. 2002b, PASP, 114, 999
Henry, G. W., Fekel, F. C., Henry, S. M., & Hall, D. S. 2000, ApJS, 130, 201
Henry, G. W., Fekel, F. C., Kaye, A. B., & Kaul, A. 2001, AJ, 122, 3383
Hesser, J. E., Moreno, H., & Ugarte, P. 1977, ApJ, 216, L31
Horaguchi, T., et al. 1994, PASJ, 46, 9
Howarth, I., & Reid, A. H. N. 1993, A&A, 279, 148
Huang, W., & Gies, D. R. 2006, ApJ, in press (astro-ph/0510720)
Hummel, W. 2000, in ASP Conf. Ser. 214, The Be Phenomenon in Early-Type Stars, ed. M. Smith, H. Henrichs, & J. Fabregat (San Francisco: ASP), 396
Hunger, K., & Groote, D. 1999, A&A, 351, 554
Khokhlova, V. L., Vasilchenko, D. V., Stepanov, V. V., & Romanyuk, I. I. 2000, Astrophys. Lett., 26, 177
Krticka, K., Mikulasek, Z., Zverko, J., & Ziznovsky, J. 2006, in ASP Conf. Ser., Active OB Stars: Laboratories for Stellar & Circumstellar Physics, ed. S. Stefl, S. Owocki, & A. Okazaki (San Francisco: ASP), in press
Lopes de Oliveiro, R., & Motch, C. 2006, A&A, in press (astro-ph/0603098)
Lyubimkov, L. S., Rostopchin, S. I., & Lambert, D. L. 2004, MNRAS, 351, 745
Marchenko, S. V., et al. 1998, A&A, 331, 1022
Mikulasek, Z., Krticka, J., et al. 2006, in ASP Conf. Ser., Active OB Stars: Laboratories for Stellar & Circumstellar Physics, ed. S. Stefl, S. Owocki, & A. Okazaki (San Francisco: ASP), in press
Miroschnichenko, A., Bjorkman, K., & Krugov, V. 2002, PASP, 114, 1226
Motch, C., Lopes de Oliveira, R., Negueruela, I., Haberl, F., & Janot-Pacheco, E. 2006, in ASP Conf. Ser., Active OB Stars: Laboratories for Stellar & Circumstellar Physics, ed. S. Stefl, S. Owocki, & A. Okazaki (San Francisco: ASP), in press
Neiner, C., et al. 2003, A&A, 409, 275
Okazaki, A. T., & Negueruela, I. 2001, A&A, 377, 161
Pamyatnykh, A. 1999, Acta Astron., 49, 119
Perryman, M. 1997, The *Hipparcos* and Tycho Catalogues (ESA SP-1200; Noordwijk: ESA)
Quirrenbach, A., et al. 1997, ApJ, 479, 477
Reid, A. H. N., et al. 1993, ApJ, 417, 320
Robinson, R. D., & Smith, M. A. 2000, ApJ, 540, 474
Robinson, R. D., Smith, M. A., & Henry, G. W. 2002, ApJ, 575, 435
Shore, S. A., & Brown, D. N. 1990, ApJ, 365, 665
Smith, M. A. 1995, ApJ, 442, 812
Smith, M. A., & Balona, L. A. 2006, ApJ, 640, 491
Smith, M. A., & Fullerton, A. F. 2005, PASP, 117, 13
Smith, M. A., & Groote, D. 2001, A&A, 372, 208
Smith, M. A., & Robinson, R. D. 1999, ApJ, 517, 866
Smith, M. A., Robinson, R. D., & Corbet, R. H. D. 1998a, ApJ, 503, 877
Smith, M. A., Robinson, R. D., & Hatzes, A. P. 1998b, ApJ, 507, 945
Spruit, H. C., Stehle, R., & Papaloizou, J. C. B. 1995, MNRAS, 275, 1223
Stehle, R., & Spruit, H. C. 2001, MNRAS, 323, 587
Thompson, I. B., & Landstreet, J. D. 1985, ApJ, 289, L9
Tycner, C., et al. 2004, AJ, 127, 1194
ud-Doula, A., & Owocki, S. P. 2002, ApJ, 576, 413
Vaníček, P. 1971, Ap&SS, 12, 10
Waters, L. B., Coté, J., & Lamers, H. J. 1987, A&A, 185, 206
Yang, S., Ninkov, Z., & Walker, G. A. 1988, PASP, 100, 233
Zorec, J., Frémat, Y., & Cidale, L. 2005, A&A, 441, 235